

Investigation of the Bond Strength Between Existing Concrete Substrate and UHPC as a Repair Material

Ahmed F. AlHallaq, Bassam A. Tayeh, Samir Shihada

Abstract: The performance of any repaired concrete structure, depends on the quality of the interfacial transition zone of the composite system formed by the repair material and the existing concrete substrate. The main aim of this paper is to evaluate the bonding behavior between normal strength concrete (NSC) substrate as an old concrete and Ultra High Performance Concrete (UHPC) as a repair material. In order to assess the bond behavior, standard slant shear test and splitting tensile test were carried out. The relation between surface roughness and bond strength in shear and indirect tension for different surfaces roughness has been assessed. The old concrete surfaces were roughened by mechanical wire brush, scarifying using an electrical grinder, scabbling by a mechanical drill and as cast without roughening. Analysis of the results indicates that bond strength increases when UHPC is used for shear and tension alike. For the scabbling technique, the shear strength yields values 251.8% higher than the those for as cast surface and 153% for tension strength. In addition, UHPC show advantages that qualify it for repairing and strengthening techniques including adding a new concrete to the existing concrete substrate. In general, rough surface preparation leads to a higher bond strength. R_a coefficient is a representative parameter and related to the bond strength, particularly, for shear strength. Finally, the results showed that tension strength is less sensitive to the surface roughness level and more proportional to the repair material strength.

Keywords: Bond strength; Concrete overlay; Old concrete; Slant shear test; Splitting test; Silica fume; Substrate; Surface roughness; Ultra High Performance Concrete,

I. INTRODUCTION

A large number of existing concrete structures worldwide is in urgent need of effective and durable repair. However, up to half of all concrete repairs are estimated to fail [1, 2]. Approximately, three-fourths of the failures can be attributed to the lack of durability. This inadequate performance is often ascribed to the lack of a reliable and perfect bond [3]. Researchers have attempted to identify ways to improve the durability of repaired concretes. The interfacial transition zone between new and old concrete is the weakest [4-6]. Good adhesion and bonding, at interfaces in concrete structures, is important for safety, durability, and better resistance against penetration of harmful substances [7-9].

Revised Version Manuscript Received on February 27, 2017.

Ahmed F. Al Hallaqa, Department of Civil Engineering, Islamic University of Gaza, Gaza, Palestine. E-mail: ahmed-alhallaq@hotmail.com

Bassam A. Tayeh, Department of Buildings Technology Engineering, University College of Applied Sciences, Gaza, Palestine. E-mail: btayeh@iugaza.edu.ps

Samir Shihada, Department of Civil Engineering, Islamic University of Gaza, Gaza, Palestine. E-mail: sshihada@iugaza.edu.ps

The adhesion of concrete repair onto an existing substrate is a complex phenomenon that involves different types of bonds. Such bonds include the chemical bond (chemical reaction between the substrate and the repair material), mechanical bond (associated with the interpenetration of the repair material into the roughness and porosity of the substrate, resulting in mechanical anchorage), and physical bond (related to the van der Waals and surface tension forces) [10, 11].

The improved durability and high compressive strength of ultra-high-performance fiber-reinforced concrete suggest its potential as a conventional overlay material and solution. However, this application can only be ensured by a strong mechanical bond between the ultra-high-performance fiber-reinforced concrete as an overlay material and the ordinary concrete as a substrate [12]. A number of studies have used ultra-high-performance fiber-reinforced concrete as a repair or composite material to strengthen ordinary concrete structural members. However, limited information on the behavior of the bond between ultra-high-performance fiber-reinforced concrete as a repair material and old concrete substrate is available.

The main objective of this study is to evaluate the bonding behavior between normal strength concrete (NSC) substrate as an old concrete and Ultra High Performance Concrete (UHPC) as repair material. In order to assess the bond behavior, standard slant shear and splitting tensile tests were carried out. The relation between surface roughness and bond strength for shear as well as indirect tension for different surface roughness has been evaluated.

II. EXPERIMENTAL PROGRAM

Two different concrete grades were used in this study, one being Grade-40 normal strength concrete and the other is Grade-120 UHPC. This research includes 48 specimens with different surface profiles which are tested by splitting and slant shear tests as shown in Figure 1.

2.1. Normal Strength Concrete

Normal strength concrete will be used as original substrata material; because, it is commonly used as a structural material in concrete buildings around the world. Normal strength concrete is a composite of aggregate, water, and cement. Table 1 shows the mix proportions which are used in this study [13]. These proportions can achieve a compressive strength of 33 MPa for standard testing cylinder.

2.2. UHPC Properties

UHPC is used as a repair material in this research. The average strength of UHPC is 112

Investigation of the Bond Strength Between Existing Concrete Substrate and UHPC as a Repair Material

MPa. The composition used, in this research, included High Strength Portland Cement CEM I 52.2R. This cement is manufactured by Nesher Cement, Inc. of Israel which conforms to ASTM C150 (2009) [14]. The nominal size of crushed basalt ranges from 0.6 to 6.3 mm, while that of quartz sand is in the range of 0.2 to 0.4 mm. The specific gravity is 2.80 and absorption is 1.48% for basalt. For quartz, the specific gravity is 2.66 and the absorption is 0.62%. Crushed quartz sand of a maximum size of 150 μm is used as very fine aggregate. The very fine particles have sizes ranging from 0.1 to 10 μm to the gaps between the cement grains while the larger particles have sizes ranging from 10 to 150 μm to fill the gaps between the fine aggregate grains resulting in much denser matrix. Gray silica fume with SiO₂ as main chemical component (95%), which conforms to the requirement of ASTM C1240-05 (2005) [15] is used. In addition, a superplasticizer PLAST_B101P, manufactured by YASMO MISR company of is used to ensure suitable workability. The mix design is shown in Table 4.

The previous proportions can achieve a compressive strength of 112 MPa for standard testing cylinder [13].

2.3. Specimen Preparation

2.3.1. Specimen Geometry

The adopted geometry for slant shear test is a 0.15 m x 0.15 m x 0.3 m composite prism, with an interface of approximately 60° to the horizontal, Figure 2.a. For splitting test, the specimens are composite cylinders and the adopted geometry is 0.15 m in diameter and 0.15 m in length, Figure 2.b. These composite specimens are prepared to be tested under compression.

2.3.2. Original Concrete Preparation

The pervious normal strength concrete mix is used to form the substrata. It is placed in lubricated half piece of cylinder specimen mold for splitting test with good compaction. For slant shear test, a wood prism form with fair face is used.

For the first seven days of casting, the specimens are left in the molds and covered by plastic sheets as a curing method. These specimens are removed from the molds and left under the natural temperature (23 ± 4 °C) for 120 days.

2.3.3. Substrata Surface Preparation

After 127 days of casting, substrata specimens, for both slant shear and splitting tests, are treated using;

- As-cast: is obtained by casting substrata surface against steel formwork,
- mechanical wire brush for 10 min/m²,
- scarifying was conducted by an electrical grinder to obtain a grid of parallel groves lines in two dimensions and random groves,
- scabbling by using a mechanical drill to obtain a surface partially chipped.
- Figure 3 shows the surfaces which were prepared using a wire brush and random scarifying.

2.4. Repair Material Placement

After the surface treatments are done, the substrata specimens are fully submersed in water for 24 hours before casting the repair material. This is to avoid the loss of

mixing water of the repair material by absorption from the substrata specimens.

The molds are prepared to contain substrata specimens and the cast repair materials casting. The remainder of the mold is filled with the repair material with good compaction, as shown in Figure 4.

As a curing method prior to demolding, the molds are covered by plastic sheets after casting in the laboratory air at 23 ± 4 °C for 7 days. Then, the specimens are demolded and cured in a saturated water at 23 ± 2 °C for an additional 21 days.

2.5. Material Strength

The compression strength test was conducted, on the same day, of the bond strength test for substrata and repair material specimens. The standard cylinder specimens which are 30 cm in length and 15 cm in diameter are used to determine the compressive strength of the substrata and the repair material, Figure 5.

2.6. Slant Shear Test

Slant shear test measures the bond strength under a state of stress that combines shear and compression. The slant shear test uses a square prism sample made of two identical halves bonded at 30° and tested under axial compression. During loading, the interface surface is under combined compression and shear stresses.

The nominal shear strength between the concrete over layer can be calculated as follows [16]:

$$\text{slant shear strength} = \frac{P}{\text{slant area}}$$

Where:

P is the maximum load carried by the composite specimen at failure in Newtons, and

slant area is the total slant contact area between substrata and repair material.

2.7. Splitting Tensile Test

This research uses the ASTM C496 [17] standard test method as a general guide and developed a splitting test for composite cylinders, constructed with one-half concrete and one-half repair material. The tensile bond strength between the substrata and the repair material is measured through the splitting strength of the composite cylinder.

The splitting tensile strength is calculated by the following equation:

$$\sigma = \frac{2P}{\pi A}$$

Where:

σ is splitting tensile strength in MPa, P is Maximum load carried by the composite specimen at failure in N and A is the area of bond plane in mm².

2.8. Surface Roughness Evaluation

In order to study the effect of surface roughness on the bond between the repair material and the concrete substrate, the roughness of the surface needs to be measured. To evaluate the surface roughness, the specimens surfaces were mapped by the handmade profile meter. A two dimensional profile 10cm long was prepared 3 times in different locations on the surface for each specimen, shown in

Figure 6. In this research, the surface roughness will be described using R_a coefficient, since this coefficient was used in most reviewed literature. This will allow comparing the results of this study with previous literatures. The average roughness, R_a , shown in Figure 7, is given by:

$$R_a = \frac{1}{l} \int_0^l |z(x)| dx$$

where l is the evaluation length, and $z(x)$ is the profile height at position x .

Other roughness coefficients such as mean, R_z , and R_{max} also will be calculated.

The mean peak-to-valley height, R_z , shown in Figure 8, is given by [18]:

$$R_z = \frac{1}{5} \sum_{i=1}^5 Z_i$$

Where Z_i is the peak-to-valley height in each cut-off length [18]:

$$R_{max} = \max\{Z_i\}$$

Where Z_i is the peak-to-valley height.

Regarding the previous equations, the roughness coefficients; mean, R_a , R_z , and R_{max} were calculated automatically using an Excel sheet that is prepared by the researchers.

III. RESULTS & DISCUSSION

Table 3 presents slant shear test results; mean shear strength, standard deviation, and mode of failure for each surface treatment technique. For splitting test, Table 4 presents the previous results but for tension strength. As shown in Table 3, the scabbling technique presents the highest shear strength with fully monolithic failure. On the other hand, fair face surface presents the lowest value of shear strength, since the fair face surface strength depends on the bond provided by the thin layer between substrata and repair material which is gained from cement paste strength. In contrast, the scabbling technique depends on the shear strength of repair material that fills the holes in the substrata surface besides to the thin cement paste layer strength.

As shown in Figure 9, it is obvious that, the scabbling technique gives the highest shear strength values compared to the other techniques with values 251.8% higher than those for fair face strength. The second highest is scarifying-grid spacing 30mm technique which gives values 196.4% higher than the fair face strength. All techniques give shear strengths higher than the fair face since the increase of the surface roughness leads to increase the contact surface area between the two materials.

Table 4 presents the results of tension strength. The results showed that the random scarifying technique gives the highest tension strength (5.4 MPa), 80% higher than the fair face strength. On the other hand, scabbling gives 4.6 MPa tension strength. This is, inversely, in shear strength and it may be explained by scabbling the groves is vertical to the

surface. So, in tension test, these groves are subject to shear stress, with shear strength is higher than tension strength.

The tremendous enhancement in the shear and splitting bond strength could be generally attributed to greater adhesion and interlocking between the UHPC and the roughened old concrete substrate surfaces. This is, particularly true, for the scabbling technique samples where the roughened or textured hardened old concrete substrate matrix and the, partially, exposed aggregates promote superior adhesion concomitant with excellent interlocking with the UHPC which ultimately contribute to exceptional interfacial shear bond strength of the composite. Here, the ability of silica fume is to improve the transition zone in concrete through its eminent micro-filler effect and outstanding pozzolanic reactivity [19-22]. Also, it played a pivotal role in enhancing the interfacial bond of the composite. It is also possible that the exposed and textured matrix of the NSC substrate could have provided a ready source of $Ca(OH)_2$ for immediate pozzolanic reaction to occur with silica fume from the UHPC. Hence, establishing is not only a mechanical bond but also a chemical bond at the interface of the composite, a combination that could be termed as “mechano-chemical” bond

Table 5 shows the average value of roughness coefficients; R_a , R_z , and R_{max} for each surface treatment techniques. Figure 11 shows the relation between the roughness coefficient R_a and shear strength which is directly proportional. As shown in previous studies [23-25], bond strength depends on the method used to promote roughness of the substrate surface. Previous studies have shown that the jack-hammer preparation technique is potentially harmful for the concrete substrate superficial layer. Probably, this explains why wire brush gives shear strength values more than the general trend in Figure 11. As a result, increasing the groove depth and width, without damaging the substrate superficial layer can increase the shear strength and this is similar to a finger print phenomenon.

Figure 12 shows the relation between the roughness coefficient R_a and tension strength. The linear regression indicates that the effect of surface roughness is insignificant according to the slope of regression line in comparison with Figure 11. Coefficient of determination, R_a equal to 0.34. Statically, it means the linear regression is not representative for this data. In other words, surface roughness, presented in R_a coefficient, is not compatible with tension strength. This indicates that tension strength is more related to the cementation of the repair material. This result is in a good agreement with the results obtained by [26, 27].

From the above analysis, one can conclude that increasing surface roughness enhances bond strength in shear significantly and proportionally up to 250%. But for tension strength, the effect of roughness will be less significant and just improves the tension strength by about 80%. This is clearly presented by the slop of linear regression of Figure 11 and Figure 12 and coefficient of determination, R_a , where the slopes are 9.1 and 1.3 for shear and tension strength respectively and coefficients of determination are 0.7 and 0.3 for shear and tension strength, respectively.

IV. CONCLUSIONS

This research investigated the effects of using UHPC as a repair material on bond strength with old concrete layers. The old concrete surfaces were roughed by mechanical wire brush, scarifying using by an electrical grinder, scabbling using a mechanical drill and left as cast against smooth framework. The following conclusions are stated:

- (1) The results showed that to ensure efficient bonding between concrete substrate surfaces and overlay materials, the substrate surface preparation is necessary since all the surface preparation methods resulted in higher bond strengths related to those achieved by the fair surface control.
- (2) The bond strength in the slant shear test is very high, as the interfacial failure occurred after the damage of the NSC substrate. The NSC substrate initially exhibited cracking and crushing prior to interfacial failure.
- (3) The scabbling technique provided the highest shear strengths with full monolithic failure. Since the bond strength is obviously stronger than the NSC substrate given that the failure occurred in the NSC substrate without interfacial separation or debonding between the NSC substrate and UHPC.
- (4) The results of splitting tensile test show that the failure mostly occurred in the NSC substrate. This means that UHPC bonded very strongly and efficiently with the NSC substrate where the wire brush and scabbling techniques behave almost monolithically
- (5) R_a coefficient is a representative parameter and related to the bond strength particularly, in shear strength. The results showed that tension strength is less sensitive to the surface roughness level and more proportional to the repair material strength.

ACKNOWLEDGMENTS

The authors are grateful to Research and Postgraduate Affairs at Islamic University of Gaza for providing the financial support. Special thanks are due to the staff of the Islamic University of Gaza (IUG) Soil and Materials Lab for their help during the sample preparation and testing.

REFERENCES

1. Mather, B. and J. Warner. Why do Concrete Repairs Fail? Interview held at University of Wisconsin, Madison Engineering Professional Development, MD, WI, <http://epdweb.engr.wisc.edu/AEC_Articles/07_Concrete_Repair_text.html>. 2003 Jan., 2012].
2. Rahman, A., et al., State-of-the-art review of interface bond testing devices for pavement layers: toward the standardization procedure. *Journal of Adhesion Science and Technology*, 2016: p. 1-18.
3. Sanchez-Silva, M., G.-A. Klutke, and D.V. Rosowsky, Life-cycle performance of structures subject to multiple deterioration mechanisms. *Structural Safety*, 2011. 33(3): p. 206-217.
4. Espeche, A.D. and J. León, Estimation of bond strength envelopes for old-to-new concrete interfaces based on a cylinder splitting test. *Construction and Building Materials*, 2011. 25(3): p. 1222-1235.
5. Rameg, P. and H.C. Khne, Investigations on the performance of concrete repair mortars in composite specimen tests., in International Conference on Concrete Repair, Rehabilitation and Retrofitting III (ICCRRR 2012), 02-05 September 2012. 2012: Cape Town, South Africa. p. 1046-1052.
6. Júlio, E., et al., Accuracy of design code expressions for estimating longitudinal shear strength of strengthening concrete overlays. *Engineering Structures*, 2010. 32(8): p. 2387-2393.
7. Gorst, N. and L. Clark, Effects of thaumasite on bond strength of reinforcement in concrete. *Cement and Concrete Composites*, 2003. 25(8): p. 1089-1094.
8. Santos, P.M.D. and E.N.B.S. Julio, Factors Affecting Bond between New and Old Concrete. *ACI Materials Journal*, 2011. 108(4): p. 449.
9. Kuebitz, K., Repairing and retrofitting prestressed concrete water tanks in the San Francisco Bay area. , in International Conference on Concrete Repair, Rehabilitation and Retrofitting III (ICCRRR 2012), 02-05 September 2012. 2012: Cape Town, South Africa.
10. Austin, S., P. Robins, and Y. Pan, Tensile bond testing of concrete repairs. *Materials and structures*, 1995. 28(5): p. 249-259.
11. Bissonnette, B., et al., Concrete repair and interfacial bond: Influence of surface preparation, in International Conference on Concrete Repair, Rehabilitation and Retrofitting II (ICCRRR 2009), 24-26 November 2009. 2009: Cape Town, South Africa. p. 345-350.
12. Tayeh, B.A., et al., Mechanical and permeability properties of the interface between normal concrete substrate and ultra high performance fiber concrete overlay. *Construction and Building Materials*, 2012. 36: p. 538-548.
13. Owayda, Y., Strengthening and Repair of RC Beams with Cementitious Repair Materials. 2013, Master Thesis, Islamic University in Gaza.
14. ASTM-C150/C150M, Standard Specification for Portland Cement, in American Society for Testing and Materials, West Conshohocken, PA 55555, United States. 2009.
15. ASTM-C1240, Standard Specification for Use of Silica Fume as a Mineral Admixture in Hydraulic Cement Concrete, Mortar, and Grout., in American Society for Testing and Materials, West Conshohocken, PA 19428-2959. 2000.
16. ASTM-C882, Standard Test Method for Bond Strength of Epoxy-Resin Systems Used with Concrete by Slant Shear, in American Society for Testing and Materials, West Conshohocken, PA 19428-2959, United States. 1999.
17. ASTM-C496, Standard Test Method for Splitting Tensile Strength of Cylindrical Concrete., in American Society for Testing and Materials, West Conshohocken, PA 19428-2959, United States. 1996.
18. Mummery, L., Surface texture analysis: the handbook. 2000: Hommelwerke.
19. Tayeh, B.A., et al., The role of silica fume in the adhesion of concrete restoration systems *Advanced Materials Research*, 2013. 626: p. 265-269.
20. Tayeh, B.A., et al., The Relationship between Substrate Roughness Parameters and Bond Strength of Ultra High- Performance Fiber Concrete. *Journal of Adhesion Science and Technology*, 2012.
21. Mohammadi, M., R. Moghtadaei, and N. Samani, Influence of silica fume and metakaolin with two different types of interfacial adhesives on the bond strength of repaired concrete. *Construction and Building Materials*, 2014. 51: p. 141-150.
22. Mohammed, A.N., et al., Improving the engineering and fluid transport properties of ultra-high strength concrete utilizing ultrafine palm oil fuel ash. *Journal of Advanced Concrete Technology*, 2014. 12(4): p. 127-137.
23. Grigoriadis, K., Use of laser interferometry for measuring concrete substrate roughness in patch repairs. *Automation in Construction*, 2016. 64: p. 27-35.
24. Tayeh, B.A., et al., Existing concrete textures: their effect on adhesion with fibre concrete overlay. *Proceedings of the Institution of Civil Engineers-Structures and Buildings*, 2014. 167(6): p. 355-368.
25. Tayeh, B.A., B. Abu Bakar, and M.M. Johari. Mechanical properties of old concrete-UHPFC interface. in *Concrete Repair, Rehabilitation and Retrofitting III: 3rd International Conference on Concrete Repair, Rehabilitation and Retrofitting*, ICCRRR-3, 3-5 September 2012, Cape Town, South Africa. 2012: CRC Press.
26. Perez, F., B. Bissonnette, and R. Gagné, Parameters affecting the debonding risk of bonded overlays used on reinforced concrete slab subjected to flexural loading. *Materials and structures*, 2009. 42(5): p. 645-662.
27. Abu-Tair, A., S. Rigden, and E. Burley, Testing the bond between repair materials and concrete substrate. *ACI Materials Journal*, 1996. 93(6).

REFERENCES

1. Mather, B. and J. Warner. Why do Concrete Repairs Fail? Interview held at University of Wisconsin, Madison Engineering Professional Development, MD, WI, <http://epdweb.engr.wisc.edu/AEC_Articles/07_Concrete_Repair_text.html>. 2003 Jan., 2012].
2. Rahman, A., et al., State-of-the-art review of interface bond testing devices for pavement layers: toward the standardization procedure. *Journal of Adhesion Science and Technology*, 2016: p. 1-18.
3. Sanchez-Silva, M., G.-A. Klutke, and D.V. Rosowsky, Life-cycle performance of structures subject to multiple deterioration mechanisms. *Structural Safety*, 2011. 33(3): p. 206-217.
4. Espeche, A.D. and J. León, Estimation of bond strength envelopes for old-to-new concrete interfaces based on a cylinder splitting test. *Construction and Building Materials*, 2011. 25(3): p. 1222-1235.
5. Rameg, P. and H.C. Khne, Investigations on the performance of concrete repair mortars in composite specimen tests., in International

List of Tables:

Table 1: Normal concrete strength mix proportions.

Table 2: UHPC mix proportions.

Table 3: Slant shear test results.

Table 4: Splitting test results.

Table 5: Average value of the roughness coefficients for each surface treatment techniques.

Table 3: Normal Concrete Strength Mix Proportions.

Material	Quantity (kg/m ³)
Cement CEM I 52.2R	320
Water	170
Quartz sand (0.15 - 0.4 mm)	680
Coarse aggregate (0.6 – 1.18 mm)	1200

Table 4: UHPC Mix Proportions.

Material	Quantity (Kg/m ³)
Cement CEM I 52.2R	600
Water	180
Silica fume	93
Quartz powder (0.0 - 0.15 mm)	242
Quartz sand (0.2 - 0.4 mm)	328
Basalt aggregate (0.6 – 6.3 mm)	1000
super plasticizer	18

Table 3: Slant Shear Test Results.

Treatment technique (3 specimens were tested for each technique)	Mean shear strength (MPa)	Standard deviation (MPa)	Mode of failure
Fair face	5.23	1.56	full interface separation
Wire brush	13.31	0.35	monolithic failure with partial separation
Scarifying-grid spacing 40mm	11.16	1.25	full interface separation
Scarifying-grid spacing 30mm	15.5	2.2	monolithic failure with partial separation
Random scarifying	13.6	1.36	monolithic failure with partial separation
Scabbling	18.4	1.78	monolithic failure

Table 4: Splitting Test Results.

Treatment technique (3 specimens were tested for each technique)	Mean tension strength (MPa)	Standard deviation (MPa)	Mode of failure
Fair face	3.0	0.14	no fracture
Wire brush	5.3	0.91	fracture in substrata & repair concrete
Scarifying-grid spacing 30mm	4.1	0.08	fracture in substrata
Scarifying-grid spacing 40mm	3.7	0.04	fracture in substrata
Random scarifying	5.4	1.03	no fracture
Scabbling	4.6	0.03	fracture in substrata & repair concrete

Table 5: Average Value of the Roughness Coefficients for Each Surface Treatment Techniques.

treatment technique	mean	R _a	R _z	R _{max}
Wire brush	0.54	0.32	0.58	0.98
Scarifying-grid spacing 30mm	0.32	0.59	1.31	3.55
Scarifying-grid spacing 40mm	0.44	0.44	0.70	3.50
Random scarifying	1.36	0.96	2.21	3.70
Scabbling	2.10	1.13	2.84	4.26

List of Figures:

Figure 1: Experimental Program.

Figure 2: a.(left) slant shear test specimen, b.(right) splitting test specimen geometry.

Figure 3: Wire brush and random scarifying treatment techniques.

Figure 4: Slant shear and splitting test specimens.

Figure 5: Mode of failure of UHPC cylinder.

Figure 6: Surface profile mapping.

Figure 7: Average roughness, R_a.

Investigation of the Bond Strength Between Existing Concrete Substrate and UHPC as a Repair Material

Figure 8: Mean peak-to-valley height, R_z .

Figure 9: Normalized chart of slant shear test results.

Figure 10: Normalized chart of splitting test results.

Figure 11: R_a coefficient value vs shear strength.

Figure 12: R_a coefficient value vs tension strength

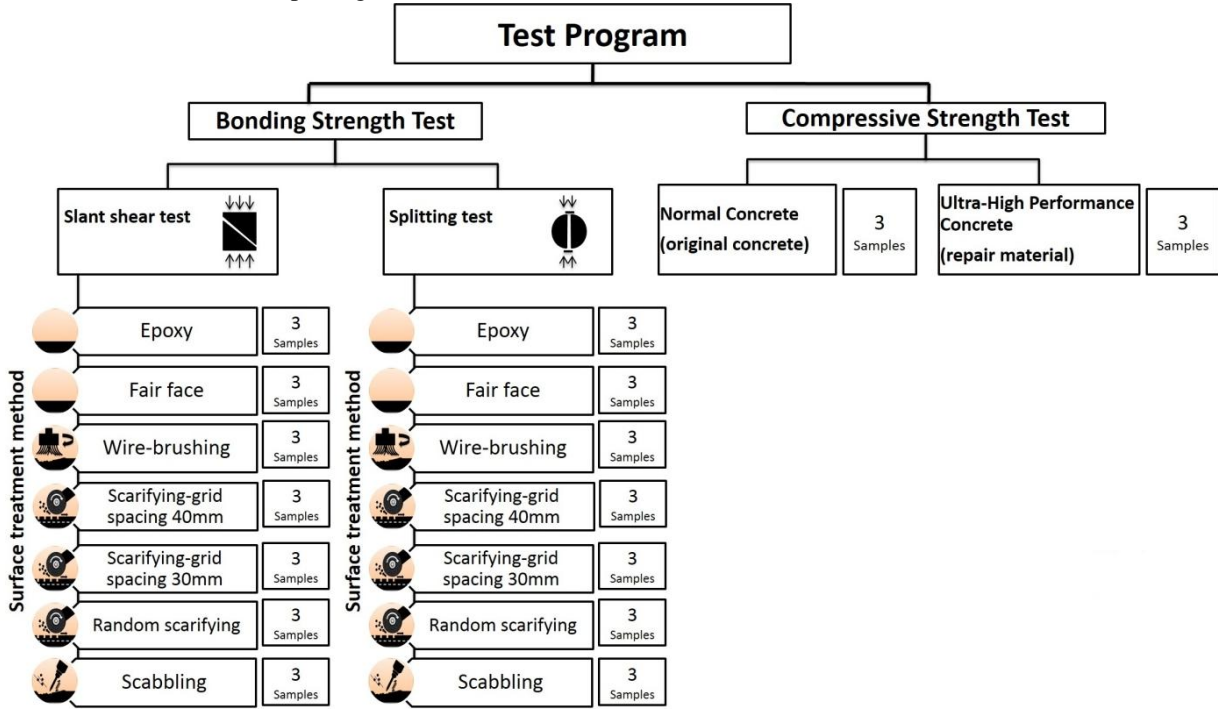


Figure 1: Experimental Program

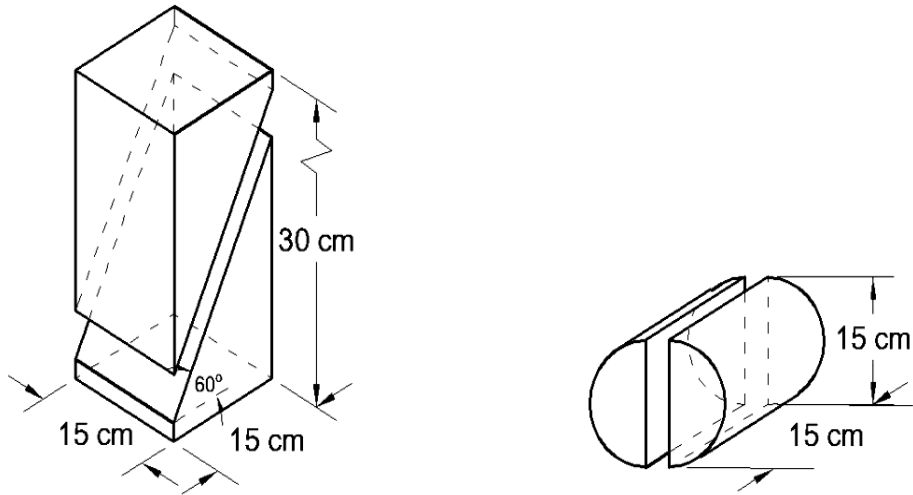


Figure 2: a.(Left) Slant Shear Test Specimen, b.(Right) Splitting Test Specimen Geometry.



Figure 3: Wire brush and Random Scarifying Treatment Techniques.



Figure 4: Slant shear and splitting test specimens.

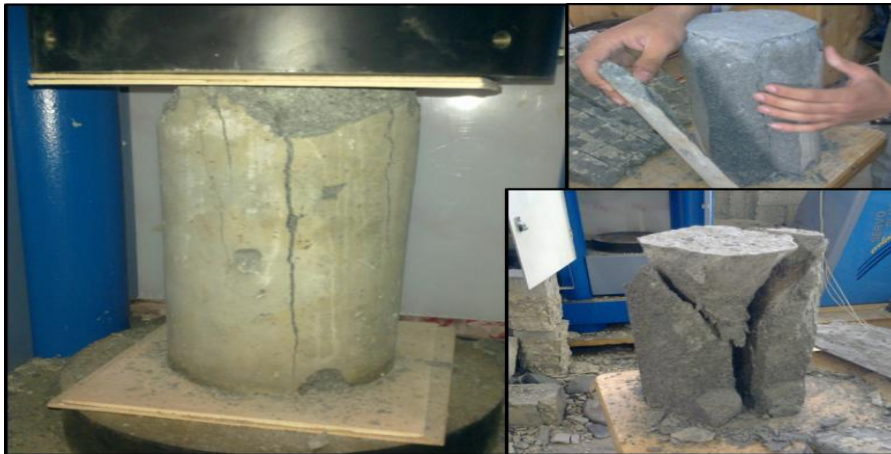


Figure 5: Mode of failure of UHPC cylinder.



Figure 6: Surface Profile Mapping.

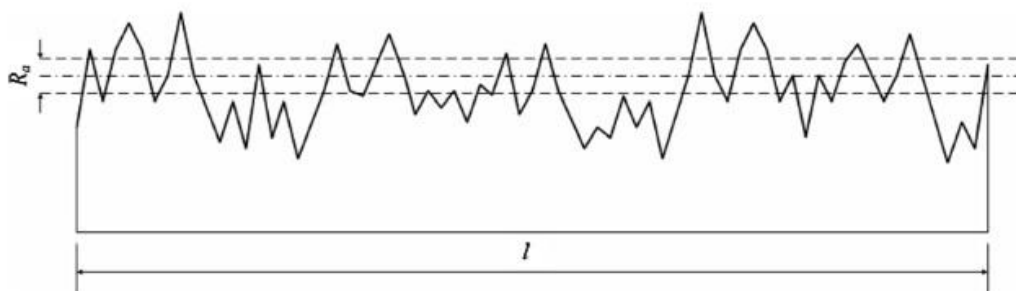


Figure 7: Average Roughness, R_a .

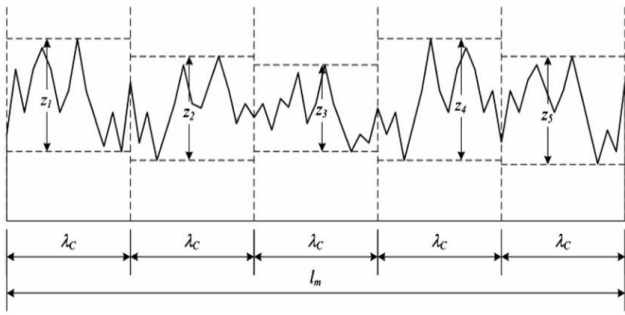


Figure 8: Mean peak-to-valley height, R_z .

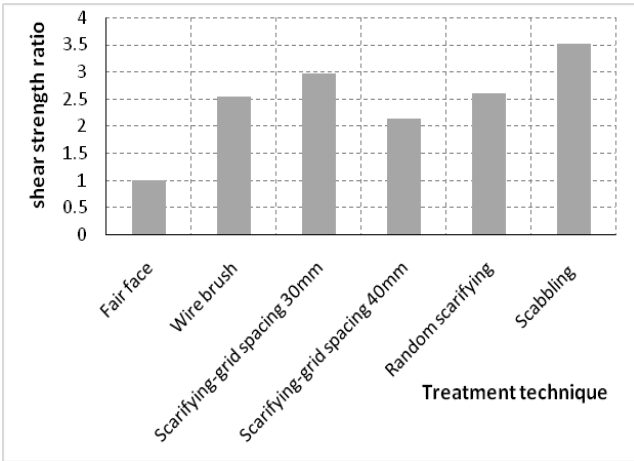


Figure 9: Normalized chart of slant shear test results.

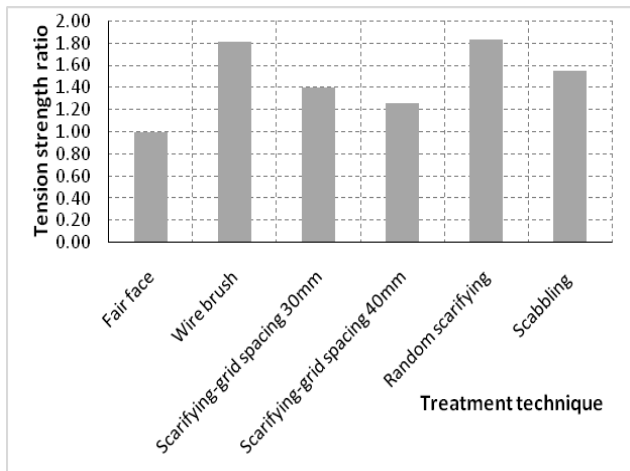


Figure 10: Normalized chart of splitting test results.

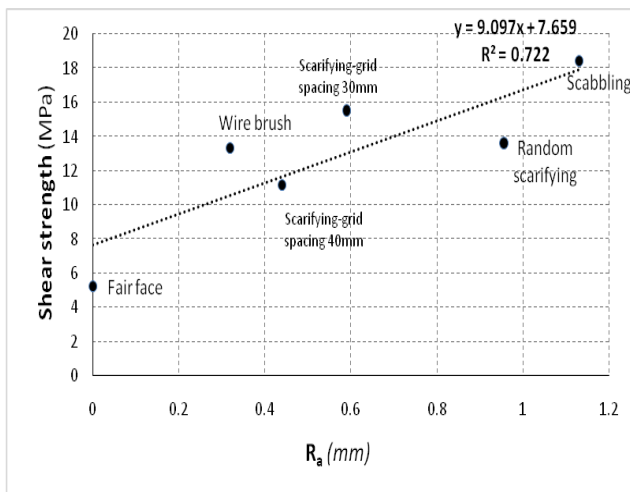


Figure 11: R_a coefficient value vs shear strength.

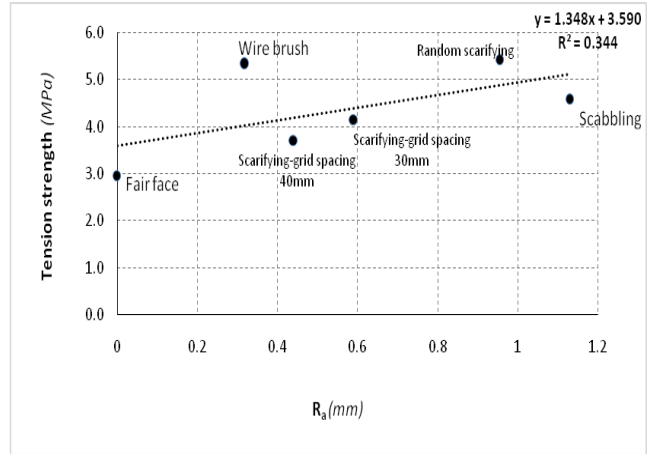


Figure 12: R_a coefficient value vs tension strength